

# A Broadband $\pm 45^\circ$ Dual-polarized Magneto-Electric Dipole Antenna for 2G/3G/LTE/5G/WiMAX Applications

Zongzheng Lu, Yufa Sun<sup>\*</sup>, Haoran Zhu, and Fei Huang

**Abstract**—A novel broadband  $\pm 45^\circ$  dual-polarized magneto-electric (ME) dipole antenna is proposed for 2G/3G/LTE/5G (3.3–3.6 GHz)/WiMAX applications. The proposed antenna has  $\Gamma$ -shaped feeding strips to impart a wide impedance bandwidth for its special structure. Stable antenna gain and radiation pattern are realized by using a rectangular box-shaped reflector instead of planar one. The antenna is fabricated and measured. The measured results show that a common impedance bandwidth is 83% with standing-wave ratio (SWR)  $\leq 1.5$  from 1.59 to 3.83 GHz and port-to-port isolation larger than 25 dB within the bandwidth. The measured antenna gains vary from 8 to 10.8 dBi and from 8 to 10.6 dBi for port 1 and port 2, respectively. The antenna has nearly symmetrical radiation patterns with low back lobe radiation both in horizontal and vertical planes, and broadside radiation patterns with narrow beam can also be obtained. The proposed antenna can be used for multiband base stations in next generation communication systems.

## 1. INTRODUCTION

In recent years, with the rapid development of modern wireless communications, there has been increased interest in wideband antenna designs. Many applications require antennas with wide impedance bandwidth, low profile, stable gain, and stable unidirectional radiation pattern with low cross polarization and low back radiation. With attractive features and advantages, the polarization-diversity technique has been widely used in modern mobile communication systems. In real implementation, a  $\pm 45^\circ$  dual-polarized antenna has been widely used in base stations because they can provide polarization diversity to reduce side effects of multipath fading and also to increase channel capacity [1]. Thus, signal reliability is enhanced. Compared with the spatial-diversity technique, the polarization-diversity technique only requires one antenna for operation, hence reducing the installation cost and space [2]. In addition, due to the coexistence of the 2G/3G/LTE/5G multi-frequency and wideband communication systems, the dual-polarized antenna with small size and broadband features is in urgent need. However, the above-mentioned antenna structure design is a challenging job for the researchers due to the mutual restriction of miniaturization and wide bandwidth.

In 2006, the magneto-electric (ME) dipole concept was first proposed [3], utilizing a combination of a planar electric dipole and an equivalent magnetic dipole realized by a shorted patch, wide bandwidth, symmetrical radiation pattern, stable gain, low cross polarization, and great front-to-back were achieved. What's more, its gain and beamwidth are not noticeably changed within its bandwidth. Then, several types of magneto-electric dipole antennas have been reported [4–7]. As a basic element, the magneto-electric dipole antenna was employed in a dual-polarization antenna [8–14]. In [10], the antenna achieved 65.9% impedance bandwidth (SWR  $\leq 2$ ) and stable radiation pattern with 3-dB beamwidth  $61.5^\circ \pm 3.5^\circ$

---

*Received 27 June 2018, Accepted 9 August 2018, Scheduled 21 August 2018*

<sup>\*</sup> Corresponding author: Yufa Sun (yfsun\_ahu@sina.com).

The authors are with the Key Lab of Intelligent Computing & Signal Processing, Ministry of Education, Anhui University, Hefei 230601, China.

at  $H$ -plane and  $62.5^\circ \pm 2.5^\circ$  at  $V$ -plane. A novel differentially-driven dual-polarized magneto-electric dipole antenna was proposed [11] in 2013, which achieved a wide impedance bandwidth of 68% (0.95 GHz to 1.92 GHz) for  $\text{SWR} \leq 2$  and unidirectional radiation pattern with 3-dB beamwidth of 62% (1.09 to 2.08 GHz). In 2015, a new dual-polarized magneto-electric dipole antenna with  $\Gamma$ -shaped feeding structure was presented [12]. The antenna exhibits good performance over the whole working bands, but its impedance bandwidth is not broad enough to support WiMAX applications at 3.5 GHz.

In this paper, a new broadband  $\pm 45^\circ$  dual-polarized magneto-electric dipole antenna for base station applications is proposed. The antenna exhibits wide impedance bandwidth, high input port isolation, stable gain, stable radiation patterns, low cross-polarization level, and low back radiation. Besides, due to the special feeding structure, the proposed antenna exhibits better performance in impedance bandwidth. Broad impedance bandwidth is achieved with SWR less than 1.5 from 1.59 to 3.83 GHz, which is suitable to serve the frequency bands of 2G/3G/LTE/5G/WiMAX communication systems. Moreover, owing to the rectangular box-shaped reflector, high and stable gain can be achieved across the operating frequency range. The proposed  $\pm 45^\circ$  dual-polarized antenna is attractive for many modern wireless communication applications.

This paper is organized as follows. In Section 2, the basic structure and operation principle of the proposed antenna are described. The experiment results of the antenna are given in Section 3, and parameter study is discussed in Section 4, followed by the conclusions presented in Section 5.

## 2. ANTENNA DESCRIPTIONS

### 2.1. Antenna Structure

The geometry of the  $\pm 45^\circ$  dual-polarized magneto-electric dipole antenna is shown in Figs. 1–3. Fig. 1 shows the perspective view of the proposed antenna. It consists of a rectangular box-shaped reflector, two pairs of horizontal planar patches, two pairs of vertical shorted patches, and a pair of orthogonal  $\Gamma$ -shaped feeding strips. The horizontal planar patch has the form of a pair of isosceles trapezoid. The rectangular box-shaped reflector with dimensions of  $130 \text{ mm}(1.17\lambda_0) \times 130 \text{ mm}(1.17\lambda_0) \times 28.8 \text{ mm}(0.26\lambda_0)$  is used to achieve relatively stable gain and better radiation performance over the passband.

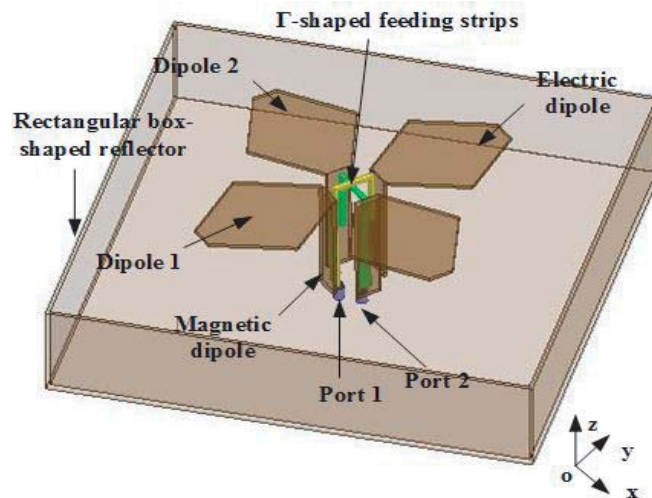


**Figure 1.** Perspective view of the  $\pm 45^\circ$  dual-polarized antenna.

The top and side views of the proposed antenna are depicted in Fig. 2. The geometry of the orthogonal  $\Gamma$ -shaped probes is depicted in Fig. 3. In fact, the  $\Gamma$ -shaped feeding structure comprises a coupling strip and a transmission line. The coupling strip is an L-shaped strip. Its horizontal portion couples electrical energy to the antenna, while the vertical portion works together with the nearest

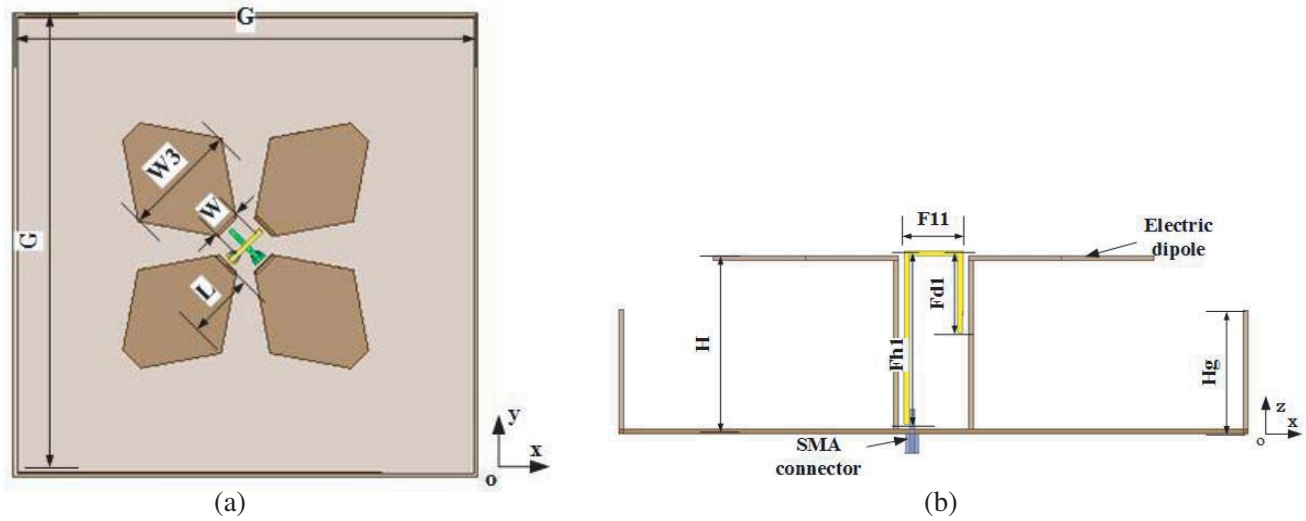


**Figure 2.** Top and side views of the  $\pm 45^\circ$  dual-polarized antenna. (a) Top view. (b) Side view.

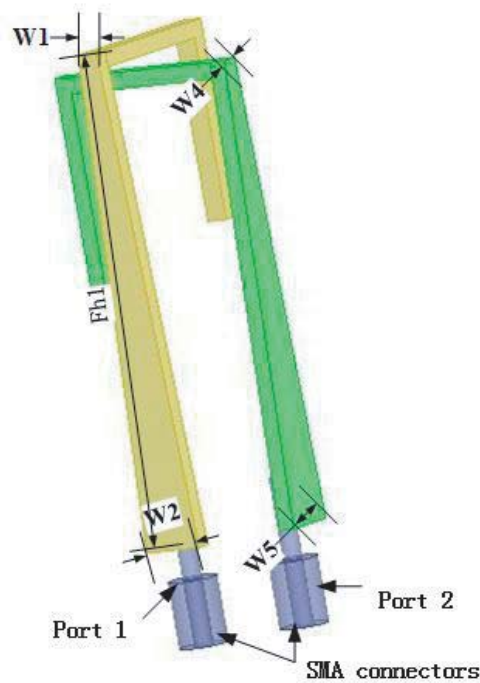


**Figure 3.** Geometry of the orthogonal  $\Gamma$ -shaped feeding strips.

vertical shorted wall patches which introduces some capacitance to compensate the inductance caused by the horizontal portion. The transmission line formed by a linear tapered metallic strip acts as an air microstrip with 1 mm separation from one of the vertical patches. The linear tapered line is used for the transmission portion to increase the impedance bandwidth which is narrower at the top (1.3 mm and 1.2 mm at each polarization) and wider at the bottom (3.7 mm and 3.7 mm at each polarization).

For dual-polarization, the  $\Gamma$ -shaped probes are located orthogonally between the vertically oriented shorted patches to produce  $\pm 45^\circ$  polarization. The taller probe (port 1) is for exciting the  $-45^\circ$  linear polarization, and the shorter probe (port 2) is for exciting the  $+45^\circ$  linear polarization. To avoid mechanical interference and for better isolation, two  $\Gamma$ -shaped probes are required to have

**Table 1.** Dimensions for the proposed dual-polarized antenna.

Parameters	$L$	$H$	$Hg$	$Fd1$	$F11$	$Fh1$	$W$
Value/mm	19 ( $0.17\lambda_0$ )	36 ( $0.32\lambda_0$ )	28.8 ( $0.26\lambda_0$ )	17 ( $0.15\lambda_0$ )	12 ( $0.11\lambda_0$ )	36 ( $0.32\lambda_0$ )	7 ( $0.06\lambda_0$ )
Parameters	$W_1$	$W_2$	$W_3$	$W_4$	$W_5$	$G$	
Value/mm	1.3 ( $0.01\lambda_0$ )	3.7 ( $0.03\lambda_0$ )	33 ( $0.30\lambda_0$ )	1.2 ( $0.01\lambda_0$ )	3.7 ( $0.03\lambda_0$ )	130 ( $1.17\lambda_0$ )	

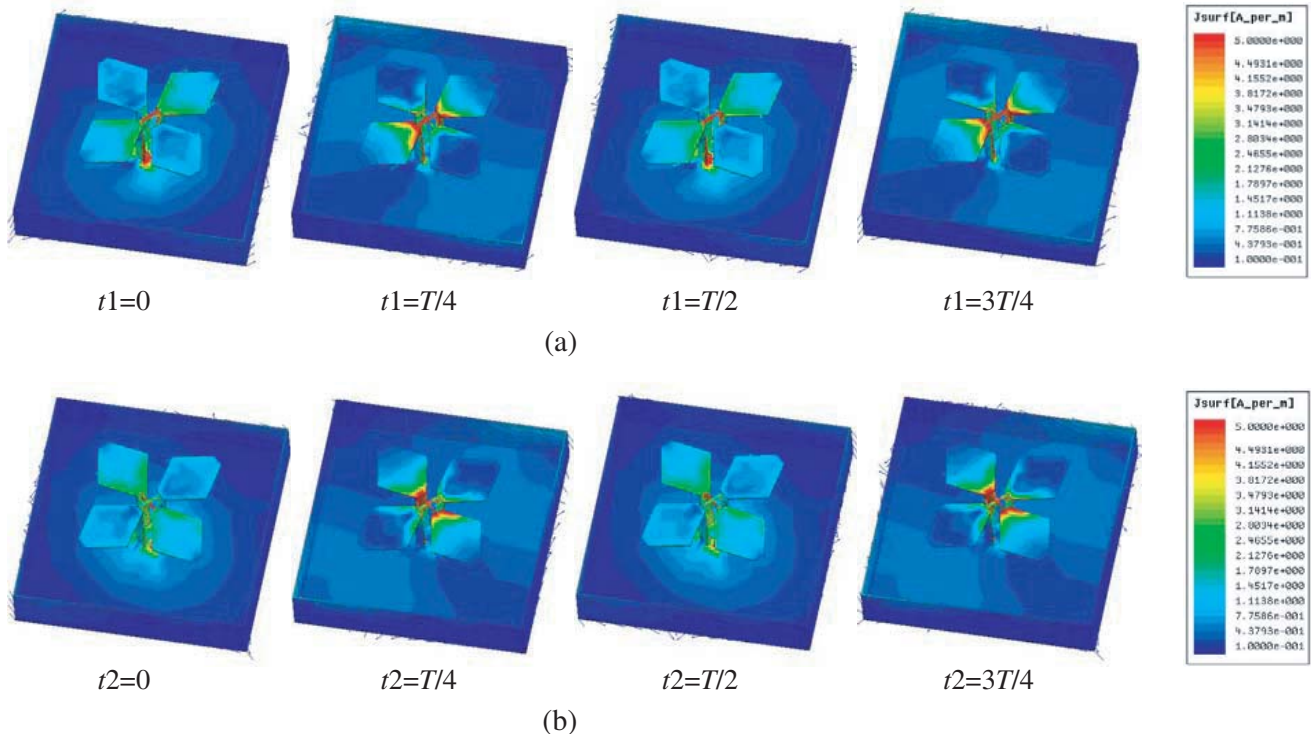
$\lambda_0$  is the wavelength referring to the center frequency of the operating band.

different heights. By using High Frequency Structure Simulator (HFSS) software, the dimensions of the configurations are simulated and optimized, and the final optimal dimension values are listed in Table 1.

In fabrication of the prototype, the proposed antenna is made of copper, and the thickness of copper patch is 1 mm. The radius of the two SMA probes is 0.6 mm, and they protrude by 4 mm above the box-shaped ground plane.

## 2.2. Antenna Operation

It is well known that the radiation pattern of an electric dipole is like a figure “8” shape in the  $E$ -plane and “O” shape in the  $H$ -plane, whereas the radiation pattern of a magnetic dipole is like a figure “O” shape in the  $E$ -plane and “8” shape in the  $H$ -plane. If an electric dipole and a magnetic dipole are excited simultaneously with proper amplitudes and phases, the radiating power can be reinforced in the broadside direction but suppressed in the back side [15]. Therefore, a uniform unidirectional radiation pattern with good radiation performances can be achieved by combining an electric dipole

**Figure 4.** Current distributions of the dual-polarized antenna. (a) Port 1. (b) Port 2.

and a magnetic dipole. In our design as depicted in Fig. 1, the antenna is a combination of two pairs of horizontal planar dipoles (electric dipole) and two pairs of vertically oriented shorted patch antennas (magnetic dipole).

For further understanding the antenna operation, the current distributions of the proposed antenna with input from the two input ports, i.e., port 1 and port 2, at time  $t_1$  and  $t_2$ , respectively, are depicted in Fig. 4. At time  $t_1 = t_2 = 0$ , the currents on the electric dipole attain maximum strength, whereas the currents on the surfaces of the magnetic dipole attain minimum strength. Thus, the currents on the electric dipole are dominated in the  $-45^\circ$  and  $+45^\circ$  directions when ports 1 and 2 are excited, respectively. At time  $t_1 = t_2 = T/4$ , the currents on the electric dipole attain minimum strength, whereas the currents on the surfaces of the magnetic dipole attain maximum strength. Therefore, the currents on the magnetic dipole are dominated in the directions of the  $-45^\circ$  and  $+45^\circ$  when ports 1 and 2 are excited, respectively. At time  $t_1 = t_2 = T/2$ , the currents on electric dipoles are dominated again with opposite direction to the currents at time  $t_1 = t_2 = 0$ . At time  $t_1 = t_2 = 3T/4$ , the currents on the magnetic dipole are dominated again with opposite direction to the currents at time  $t_1 = t_2 = T/4$ .

Hence, two degenerate modes of similar magnitude in strength are excited on the planar dipole (electric dipole) and the quarter-wave shorted patch antennas (magnetic dipole). The equivalent electric and magnetic currents are 90 degrees in phase difference and orthogonal to each other. It is expected that the proposed antenna can achieve stable gain and low back radiation over the operating frequency band.

### 3. SIMULATED AND MEASURED RESULTS

To verify the proposed design, an antenna prototype was constructed, as shown in Fig. 5. Measured results of SWRs, gains, isolation and radiation patterns were obtained by Agilent N5247A network analyzer and a SATIMO antenna measurement system.

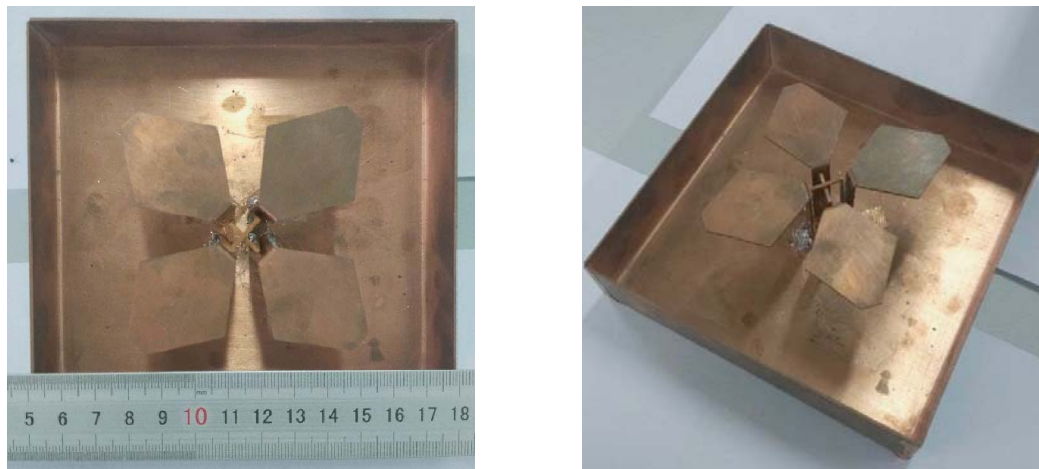


**Figure 5.** Prototype of the  $\pm 45^\circ$  dual-polarized antenna.

Figure 6 depicts simulated and measured SWRs and gains of the proposed  $\pm 45^\circ$  dual-polarized antenna. It can be seen clearly that the antenna operates from 1.59 to 3.83 GHz with a bandwidth of 83% ( $\text{SWR} \leq 1.5$ ) and from 1.59 to 3.90 GHz with a bandwidth of 84% ( $\text{SWR} \leq 1.5$ ) for ports 1 and 2, respectively. The operating frequency ranges for the two ports are slightly different due to the unequal heights and dimensions of the two orthogonal strip lines. The common bandwidth of the two ports is 83% ranging from 1.59 to 3.83 GHz. Over the operating frequency range, the measured broadside gains for port 1 and port 2 are  $9.4 \pm 1.4$  dBi and  $9.3 \pm 1.3$  dBi, respectively. Hence, the gains are relatively stable and high enough for 2G/3G/LTE/5G/WiMAX base-station communications. Fig. 7 shows the isolation between the two ports. The measured isolation between the two ports is better than 25 dB over the entire operating frequency band.

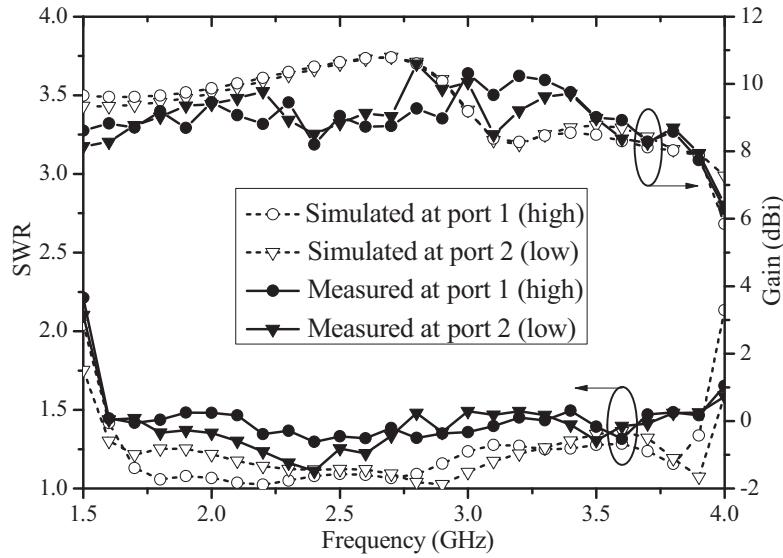


**Figure 6.** Simulated and measured SWRs and gains of the  $\pm 45^\circ$  dual-polarized antenna.

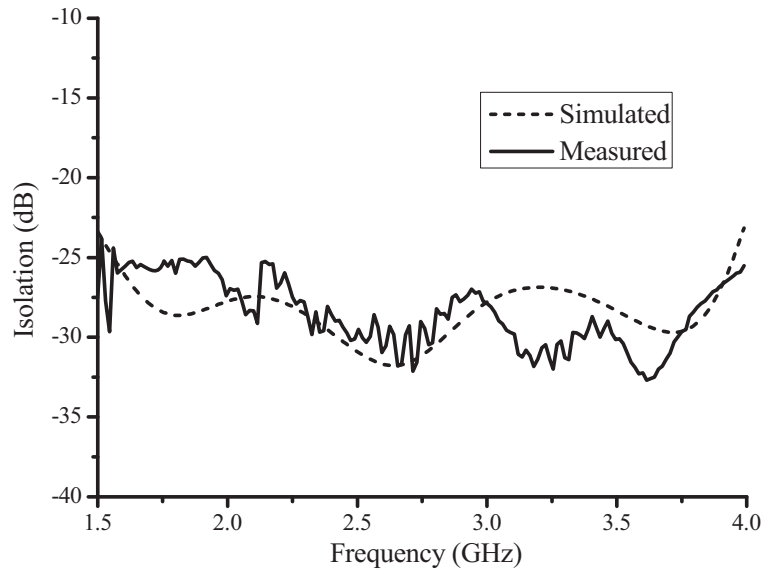


**Figure 7.** Simulated and measured isolation of the  $\pm 45^\circ$  dual-polarized antenna.

In order to investigate the reasons that the proposed antenna has such a wide impedance bandwidth clearly, a comparison between the double-polarization antenna (DPA) and the linear polarization antenna (LPA) was made. The DPA is the antenna we proposed, and the LPA is obtained simply by deleting the dipole 2 (shown in Fig. 1) from the DPA with remaining all other configurations unchanged.

Figure 8 shows the SWRs of the LPA and DPA. It can be seen that in the frequency range from 1.6 GHz to more than 3.8 GHz, the DPA has a much better impedance performance. Fig. 9 shows the current vector distribution of the DPA at 2.2 GHz when only dipole 1 is excited. It can also be found that current distribution with large magnitude appears on dipole 2. So there is strong mutual coupling between the two dipoles. As mentioned above, the only difference between the LPA and the DPA is that the LPA has only one dipole, while the DPA has two orthogonal dipoles. Therefore, the reason that the DPA has a much wider impedance bandwidth becomes clear. That the orthogonally situated dipole 2 works as a parasitic element for dipole 1 greatly extends the impedance bandwidth of the latter,

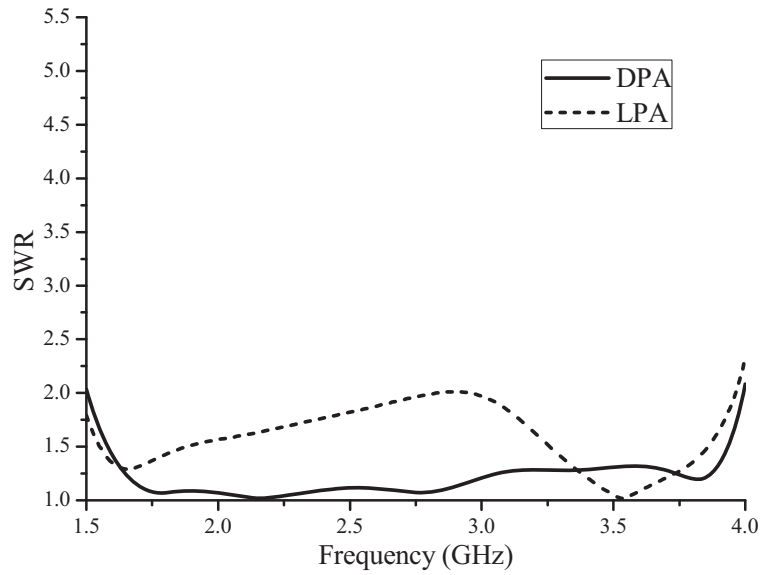


Figure 8. Simulated SWRs of the DPA and the LPA.

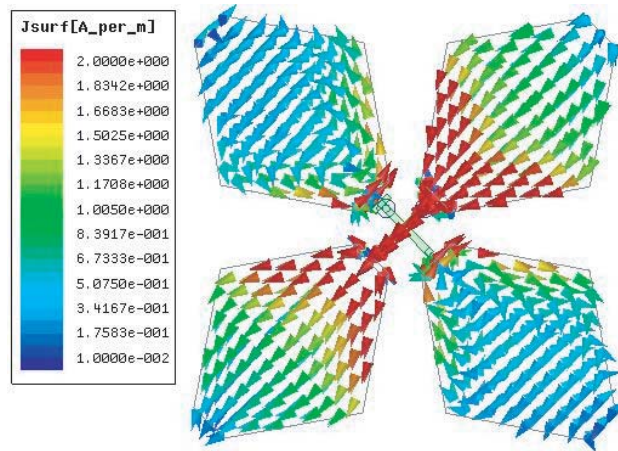
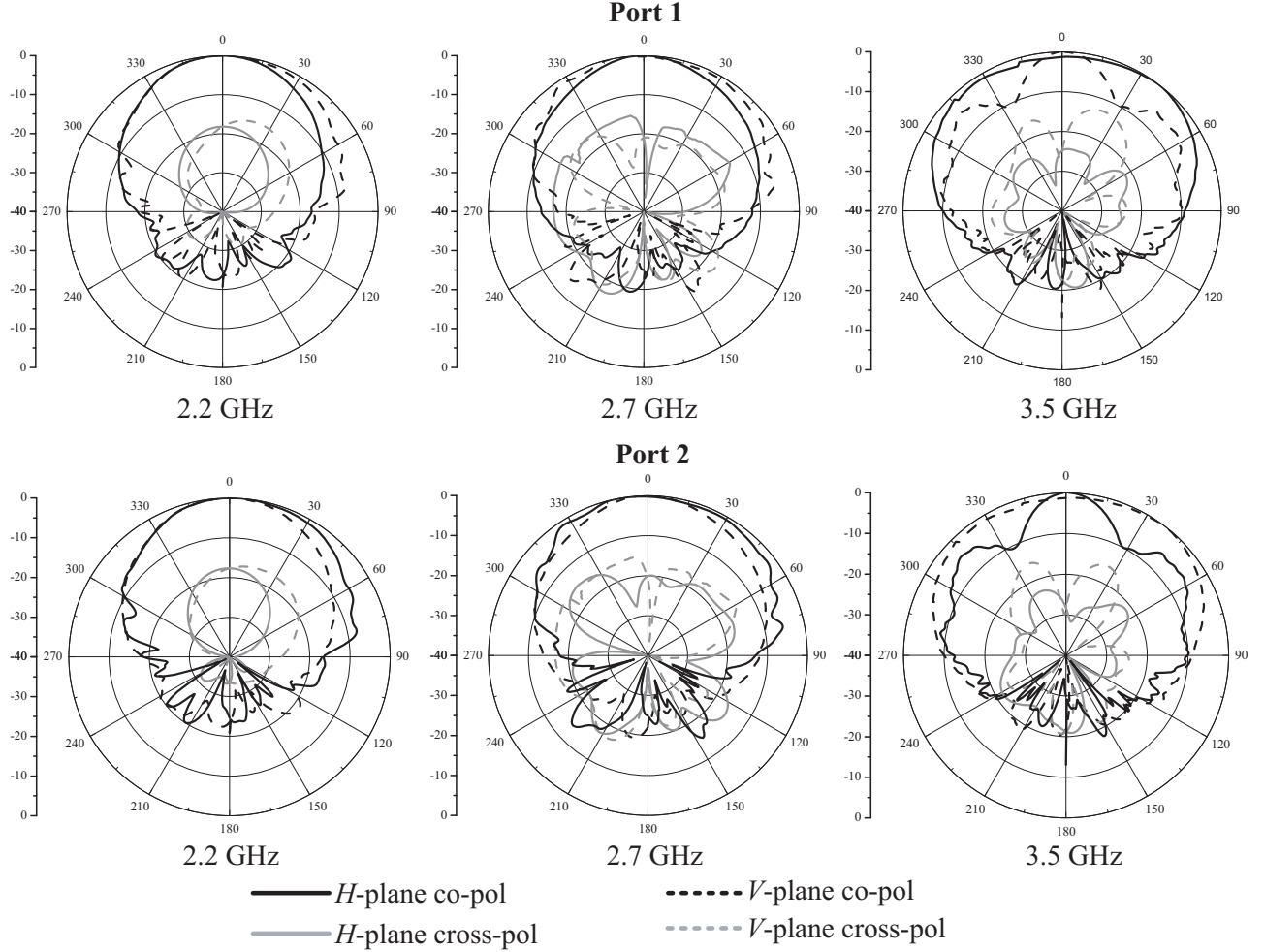


Figure 9. Current vector distribution on the DPA of 2.2 GHz at  $t = T/4$  when only the dipole 1 is excited.

due to the introducing of parasitic element, and another resonant frequency appears. And vice versa, the dipole 1 will also extend the impedance bandwidth of the dipole 2 [16]. Additionally, the electric dipole structure can lengthen the current path and expand the effective radiation area, resulting in the downward trend of the cutoff frequency and increase of the bandwidth.

The measured radiation patterns of the proposed  $\pm 45^\circ$  dual-polarized magneto-electric dipole antenna for port 1 and port 2 at frequencies of 2.2, 2.7 and 3.5 GHz are plotted in Fig. 10, which shows that the antenna has a nearly symmetric and good unidirectional radiation pattern across the entire bandwidth. Detailed measured results including the 3-dB beamwidth in both horizontal and vertical planes, and the front-to-back ratios (FBRs) at two ports are summarized in Table 2. The 3-dB beamwidths in both horizontal and vertical planes for both ports become narrower as frequency increases, due to the effect of the rectangular box-shaped reflector. Besides, the 3-dB beamwidth is influenced to high order mode at higher frequencies. The measured FBRs of the two ports are above 20 dB in most parts of the operating frequency band. The cross-polarization levels for both  $H$ - and  $V$ -planes are less than  $-18$  dB.



**Figure 10.** Measured radiation patterns of the dual-polarized antenna at frequencies of 2.2, 2.7 and 3.5 GHz.

**Table 2.** Summary of the measured radiation patterns at different frequencies.

Frequency (GHz)	Port 1 ( $-45^\circ$ polarization)			Port 2 ( $+45^\circ$ polarization)		
	3-dB beamwidth		FBR (dB)	3-dB beamwidth		FBR (dB)
	<i>H</i> -plane	<i>V</i> -plane		<i>H</i> -plane	<i>V</i> -plane	
1.8	$70.1^\circ$	$62.3^\circ$	20.7	$55.8^\circ$	$64.7^\circ$	21.6
2.0	$68.6^\circ$	$57.2^\circ$	22.9	$56.3^\circ$	$66.1^\circ$	20.4
2.2	$62.1^\circ$	$55.2^\circ$	21.8	$53.8^\circ$	$65.2^\circ$	22.6
2.5	$58.2^\circ$	$51.6^\circ$	23.7	$50.2^\circ$	$56.6^\circ$	19.6
2.7	$55.8^\circ$	$50.6^\circ$	20.1	$49.1^\circ$	$52.8^\circ$	21.2
3.0	$48.6^\circ$	$45.0^\circ$	18.7	$44.6^\circ$	$47.5^\circ$	19.5
3.5	$43.5^\circ$	$87.8^\circ$	17.4	$96.1^\circ$	$42.9^\circ$	18.3

#### 4. PARAMETRIC STUDY AND DISCUSSION

For a better understanding of how the dimensions of the antenna affect its performances, some parameters of the magneto-electric dipoles and rectangular box-shaped reflector are studied by simulation. For simplicity, only port 1 is excited, because of the symmetry of the antenna. When



one parameter is studied, the others are kept constant. The results provide a useful guideline for practical design.

#### 4.1. Effects of the ME Dipoles

The first and most important parameter was the length  $L$  of the horizontal portion of the planar dipole. It can be observed from Fig. 11 that both SWR and gain are highly sensitive to the value of  $L$ . If  $L$  is increased such that the electric dipole is enlarged, the first resonance is shifted to a lower frequency. Thus, it can be concluded that the first resonance is mainly affected by the electric dipole, and when the length of the electric dipole becomes longer, the resonant frequency obviously should move to a lower frequency according to the antenna theory. Therefore, to achieve a good impedance matching and

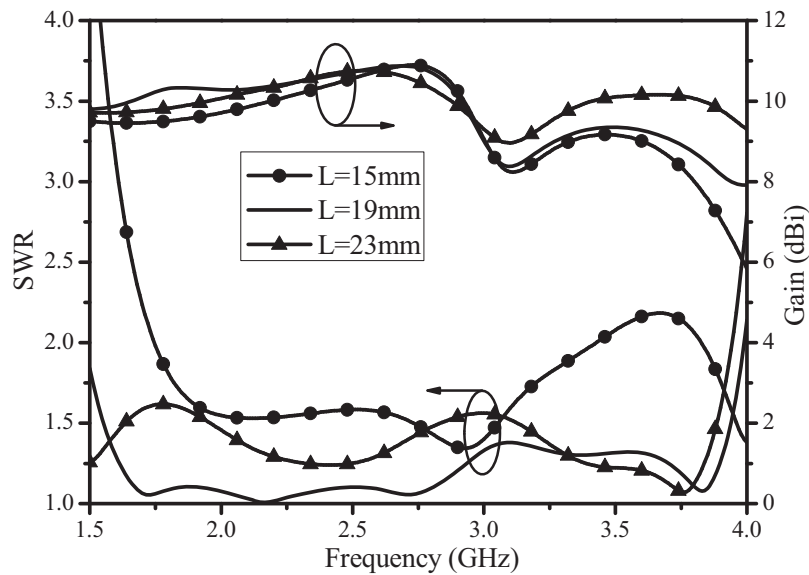


Figure 11. Effects of  $L$  on SWR and gain.

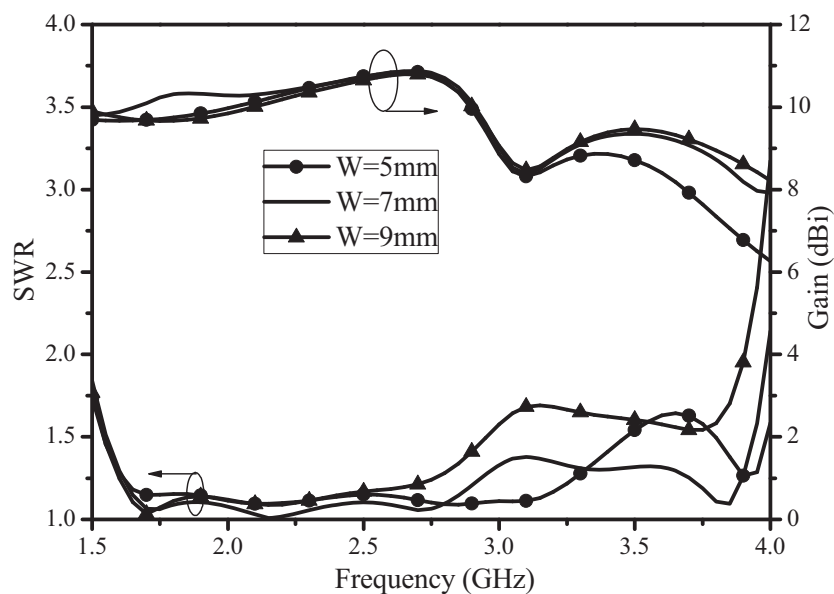


Figure 12. Effects of  $W$  on SWR and gain.

stable gain over a wide frequency band,  $L = 19$  mm was selected.

The second parameter studied was the width  $W$  of the planar dipole and vertically oriented shorted patches. Fig. 12 shows the simulated results of the SWR and gain. It can be seen that the SWR bandwidth is very sensitive to this parameter. The antenna gain and SWR at higher frequency is highly influenced by the variation of  $W$ . For the proposed prototype,  $W = 7$  mm was chosen to achieve wide impedance bandwidth and stable gain.

The third parameter studied was  $W_3$ . The effects of  $W_3$  on SWR and gain are shown in Fig. 13. It can be seen that the SWR bandwidth is very sensitive to this parameter. The antenna gain and SWR at higher frequency are highly influenced by the variation of  $W_3$ .  $W_3 = 33$  mm was chosen for stable antenna gain and good impedance matching over a wide frequency band.

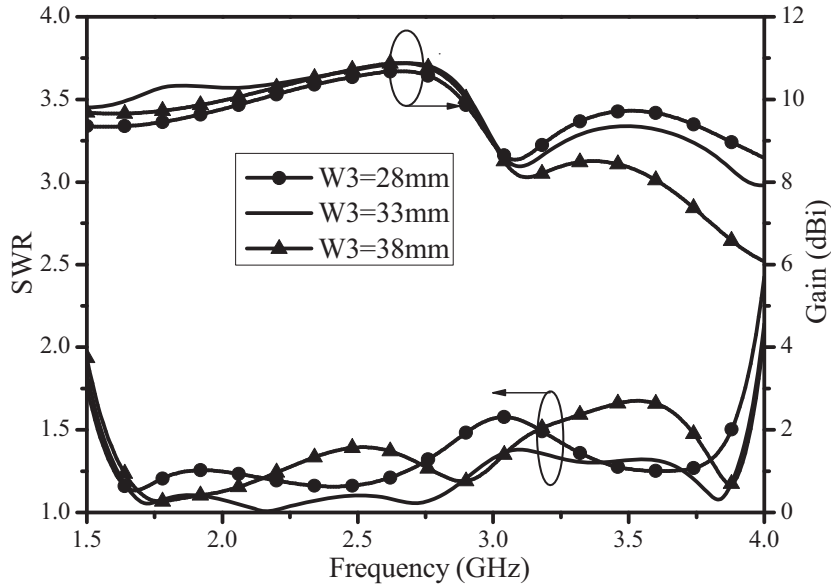


Figure 13. Effects of  $W_3$  on SWR and gain.

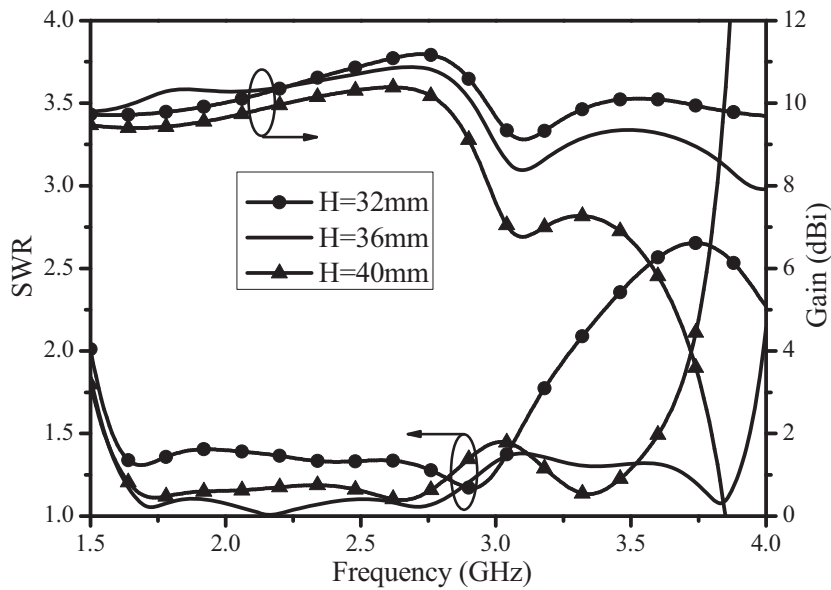


Figure 14. Effects of  $H$  on SWR and gain.

The fourth parameter studied was the height  $H$  of the antenna. The effects of  $H$  on SWR and gain are shown in Fig. 14. It was found that the SWR and gain are sensitive to the value of  $H$ . The antenna gain and SWR at higher frequency are highly influenced by the variation of  $H$ . Therefore, to achieve a good impedance matching over a wide frequency band,  $H = 36$  mm was selected.

### 4.2. Effects of the Rectangular Box-Shaped Reflector

To achieve stable radiation patterns, a rectangular box-shaped reflector is necessary for a unidirectional antenna. To understand the usefulness of such a reflector, the antenna with a rectangular box-shaped reflector and a planar reflector was analyzed. As shown in Fig. 15, with a rectangular box-shaped reflector, the SWR is more stable, and the gain is much higher than the other. Fig. 16 depicts the simulated radiation patterns when port 1 is excited at 3.5 GHz for the dual-polarized antenna with and without metallic wall. The metallic wall improves both 3-dB beamwidth and back radiation. In short, the rectangular box-shaped reflector is conducive to improving the antenna performances.

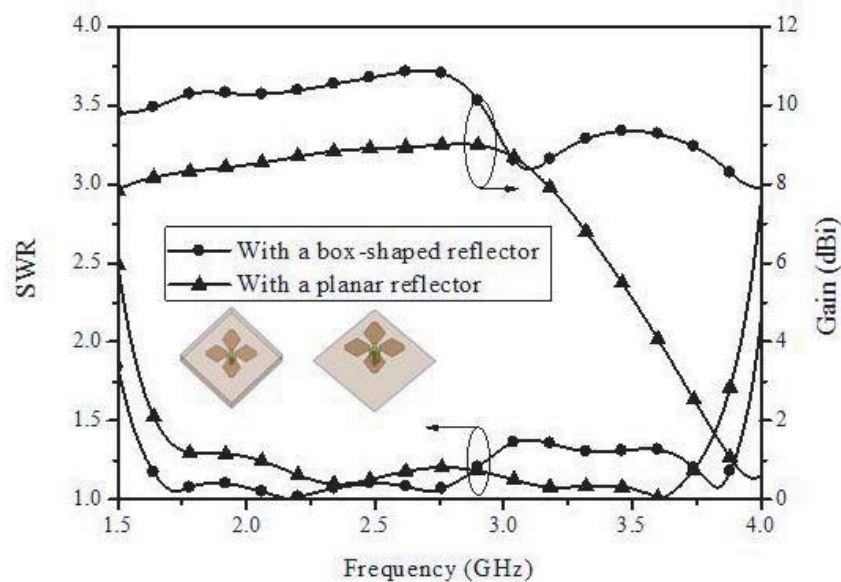


Figure 15. Effects of reflectors on SWR and gain at port 1.

### 4.3. Comparison and Discussion

Structural characteristics and performances of different kinds of dual-polarized antennas are listed in Table 3 to compare with our work. First, wider impedance bandwidth can be achieved by the proposed antenna, which can be used for 2G/3G/LTE/5G/WiMAX base stations in next generation communication systems. Moreover, better gain performance can be achieved by this paper in comparison with the designs in [12] and [16].

Table 3. Comparison between proposed and reported antennas.

Ref.	Size (mm)	BW (%)	Gain (dBi)	Feed Structure
[12]	110 × 110 × 36	48% (1.69–2.76 GHz)	7.6–9.3	Γ-shaped probes
[16]	140 × 140 × 34	45% (1.7–2.7 GHz)	7.6–8.8	Y-shaped feeding lines
This work	130 × 130 × 36	83% (1.59–3.83 GHz)	8–10.6	Special Γ-shaped feeding strips

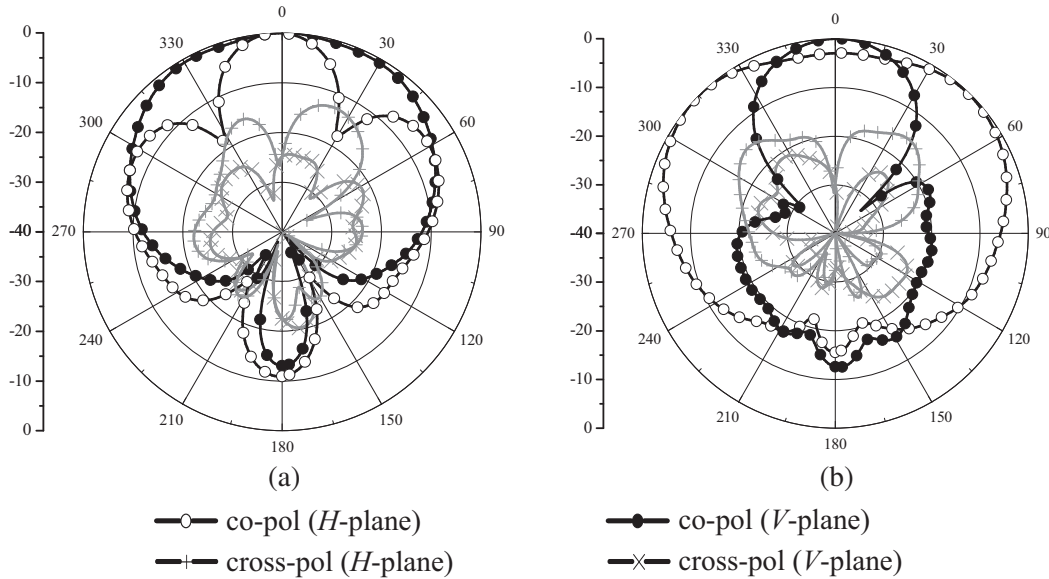


**Figure 16.** Simulated radiation patterns of the dual-polarized antenna. (a) With rectangular box-shaped reflector at 3.5 GHz. (b) With planar reflector at 3.5 GHz.

## 5. CONCLUSION

A novel broadband  $\pm 45^\circ$  dual-polarized magneto-electric dipole antenna with  $\Gamma$ -shaped feeding strips proposed for base-station communication is designed, fabricated, and measured. Measured results revealed that the proposed antenna exhibited an overlapped impedance bandwidth of 83% with  $\text{SWR} \leq 1.5$  from 1.59 to 3.83 GHz, and the isolation between the two ports was more than 25 dB. Other electric characteristics, such as stable and high gain, high front-to-back ratio, and symmetrical  $H$ - and  $V$ -plane radiation patterns with proper beamwidth are also obtained. Because of these excellent features, the proposed antenna is a promising candidate for modern 2G/3G/LTE/5G/WiMAX base-station communication systems.

## ACKNOWLEDGMENT

This work is supported by the National Natural Science Foundation of China under Grant 61172020.

## REFERENCES

1. Guo, Y. X., K. M. Luk, and K. F. Lee, "Broadband dual polarization patch element for cellular-phone base stations," *IEEE Transactions on Antennas & Propagation*, Vol. 50, No. 2, 251–253, 2002.
2. Turkmani, A. M. D., A. A. Arowojolu, P. A. Jefford, and C. J. Kellett, "An experimental evaluation of the performance of two-branch space and polarization diversity schemes at 1800 MHz," *IEEE Trans. Vehicular Technology*, Vol. 44, No. 2, 318–326, May 1995.
3. Luk, K. M. and H. Wong, "A new wideband unidirectional antenna element," *Int. J. Microw. Opt. Technol.*, Vol. 1, 35–44, Jun. 2006.
4. Zhang, J. R. and L. Z. Song, "Dual-polarized complementary structure antenna based on Babinet's principle," *Progress In Electromagnetics Research Letters*, Vol. 64, 29–36, 2016.
5. An, W. X., H. Wong, K.-L. Lau, S. F. Li, and Q. Xue, "Design of broadband dual-band dipole for base station antenna," *IEEE Transactions on Antennas & Propagation*, Vol. 60, No. 3, 1592–1595, Mar. 2012.

6. Luk, K. M. and B. Q. Wu, "The magneto-electric dipole — A wideband antenna for base stations in mobile communications," *Proc. IEEE*, Vol. 100, No. 7, 2297–2307, Jul. 2012.
7. He, K., S. X. Gong, and F. Gao, "A wideband dual-band magneto-electric dipole antenna with improved feeding structure," *IEEE Antennas Wirel. Propag. Lett.*, Vol. 13, 1729–1732, 2014.
8. Siu, L., H. Wong, and K. M. Luk, "A dual-polarized magneto-electric dipole with dielectric loading," *IEEE Transactions on Antennas & Propagation*, Vol. 57, No. 3, 616–623, Mar. 2009.
9. An, W. X., S. F. Li, W. J. Hong, F. Z. Han, and K. P. Chen, "Design of wideband dual-band dual-polarized dipole for base station antenna," *Journal of China Universities of Posts and Telecommunications*, Vol. 19, No. 1, 22–28, Jun. 2012.
10. Wu, B. Q. and K. M. Luk, "A broadband dual-polarized magneto-electric dipole antenna with simple feeds," *IEEE Antennas Wireless Propag. Lett.*, Vol. 8, 60–63, 2009.
11. Xue, Q., S. W. Liao, and J. H. Xu, "A differentially-driven dual-polarized magneto-electric dipole antenna," *IEEE Transactions on Antennas & Propagation*, Vol. 61, No. 3, 425–430, Jan. 2013.
12. Li, M. J. and K. M. Luk, "Wideband magneto-electric dipole antennas with dual polarization and circular polarization," *IEEE Antennas and Propagation Magazine*, Vol. 57, No. 1, 110–119, Feb. 2015.
13. Yang, L., Z. Weng, and C. Zhang, "A dual-wideband dual-polarized directional magneto-electric dipole antenna," *IEEE Transactions on Antennas & Propagation*, Vol. 59, No. 5, 1128–1133, 2017.
14. Wen, D., D. Zheng, and Q. X. Chu, "A wideband differentially-fed dual-polarized antenna with stable radiation pattern for base stations," *IEEE Transactions on Antennas & Propagation*, Vol. 65, No. 5, 2248–2255, 2017.
15. Clavin, A., "A new antenna feed having equal  $E$ - and  $H$ -plane patterns," *IRE Trans. Antennas Propag.*, Vol. 2, No. 3, 113–119, Jul. 1954.
16. Chu, Q. X., D.-L. Wen, and Y. Luo, "A broadband  $\pm 45^\circ$  dual-polarized antenna with Y-shaped feeding lines," *IEEE Transactions on Antennas & Propagation*, Vol. 63, No. 2, 483–490, Feb. 2015.